PB 80120462

REPORT NO. FRA/ORD-79/41

NUMERICAL DETERMINATION OF CONTACT PRESSURES BETWEEN CLOSELY CONFORMING WHEELS AND RAILS

TECHNICAL REPORT NO. 8

BY

B. PAUL AND J. HASHEMI

JULY 1979

PREPARED FOR THE

DEPARTMENT OF TRANSPORTATION

FEDERAL RAILROAD ADMINISTRATION
WASHINGTON, DC 20590

TECHNICAL REPORT STANDARD TITLE PAGE

1. Report No.	2. Government Accession No.	3. Recipient's Catalog No.
FRA/ORD-79/41	PB 80120462	

4. Title and Subtitle	5. Report Date
Numerical Determination of Contact Pressures Between Closely Conforming Wheels and Rails	July 1979
	6. Performing Organization Code
7. Author(s)	8. Performing Organization Report No.
B. Paul and J. Hashemi	MEAM Report 79-4
9. Performing Organization Name and Address	10. Work Unit No.
Department of Mechanical Engrg. & Applied Mechanics University of Pennsylvania - 111 Towne Building/D3 Philadelphia, PA 19104	11. Contract or Grant No. DOT-OS-60144
	13. Type of Report and Period Covered Technical Report No. 8
12. Sponsoring Agency Name and Address Department of Transportation Federal Railroad Administration 400 Seventh Street, S.W. Washington, DC 20590	14. Sponsoring Agency Code

15. Supplementary Notes

16. Abstract

A numerical method is developed for the determination of the contact pressure that arises when two elastic bodies with closely conforming non-Hertzian frictionless surfaces are pressed together. The method is a generalization of that recently developed by the authors for the case of counterformal contact, and includes a technique for automatically generating meshes that overlay the changing (load-dependent) contact patches. The method has been implemented in a computer program called CONFORM, and has been applied to problems of wheel and rail contact. The results have been verified by comparison with those generated by an independent program for the special case of relatively light wheel loading, where the contact is known a-priori to be essentially counterformal. The results given herein for a relatively heavy (but realistic) wheel loading on the throat of the flange represent the first known solution for conformal contact between a railroad wheel and rail.

17. Key Words	18. Distribution Statement
Rail wheel interaction, contact stress, conformal contact, elasticity, non-Hertzian contact	Document is available through the National Technical Information Service, Springfield, Virginia 22161

19. Security Classif. (of this report)	20. Security Classif. (of this page)	21. No. of Pages	22. Price
Unclassified	Unclassified	28	

Form DOT F 1700.7 (8-69)

TABLE OF CONTENTS

Page

1. Introduction ---------- 1

2. Formulation of the Governing Integral Equation ---------- 3

3. Discretization of the Integral Equation ---------- 8

4. Initial Candidate Contact Boundary ---------- 11

5. Mesh Generation and Contact Boundary Determination ---------- 11

6. Organization of Computer Program ---------- 14

7. Examples ---------- 17

8. Conclusions ---------- 24

References ---------- 25

Appendix A: Influence Functions for Rail and Wheel Surfaces ---------- 26

List of Related Publications ---------- 27

1. INTRODUCTION

Elastic contact stress problems are classified as Hertzian if they satisfy the following five conditions:

1. The bodies are homogeneous, isotropic, obey Hooke's law, and experience small strains and rotations (i.e., the linear theory of elasticity applies).
2. The contacting surfaces are frictionless.
3. The dimensions of the deformed contact patch remain small compared to the principal radii of the undeformed surfaces.
4. The deformations are related to the stresses in the contact zones as predicted by the linear theory of elasticity for half spaces (Boussinesq's influence functions are valid).
5. The contacting surfaces are continuous, and may be represented by second degree polynomials (quadratic surfaces) prior to deformation.

Contact stress problems are also classified as:

a. Counterformal (or antiformal), if Condition 3 is satisfied, or
b. Conformal, if Condition 3 is violated.

Until recently, there existed no general way of handling any non-Hertzian problems. However, Singh and Paul [1974] showed how to solve antiformal non-Hertzian problems using the so-called Simply Discretized (S.D.) method. This method was applied by them to relatively simple geometries. Later, Woodward and Paul [1976] extended the S.D. method to the case of conformal problems, but restricted their attention to the cases of cylinders and spheres. More recently, Paul and Hashemi [1978-a] developed a modification of the S.D. method by means of which they were able to solve antiformal contact problems for virtually arbitrary geometries. By means of a computer program COUNTACT (see Paul and Hashemi [1977]) they found the first known solutions for realistic rail and wheel profiles in antiformal contact.

The present work represents an extension of the modified S.D. method to conformal problems with quite general geometries - including that of wheel and rail profiles in closely conforming regions of the flange throat. Based upon this analysis, a computer program (called CONFORM) has been developed and reported upon by Paul and Hashemi [1978-b].

Additional references on related literature will be found in the cited papers of Singh, Paul, and Woodward in the Ph.D. dissertation of Hashemi [1979].

In the next section, we formulate the based integral equations governing conformal contact stress problems. In Section 3, we show how the Modified Simply Discretized Method can be used to solve the governing integral equation.

In Section 4 the determination of the initial candidate contact boundary is discussed. This is a necessary preliminary for the numerical method being used.

In Section 5 methods are developed for mesh generation and boundary determination which are more general and efficient than those used in the previously cited references. Section 6 briefly explains the organization of computer programs developed for this work. Examples are given in Section 7 and Conclusions are stated in Section 8.

2. FORMULATION OF THE GOVERNING INTEGRAL EQUATION

Let the two bodies of general, but closely conforming, shape be denoted as body 1 and body 2. Cartesian coordinate axes are set up with the initial contact point as common origin. Axes (x,y) lie in the tangent plane of the two surfaces at the initial contact point, with the z-axis pointing into body 2. Both surfaces are frictionless. Due to the applied loads, material points in the two bodies undergo rigid-body translation and elastic deformation.

The initial separation of points on the two bodies with common (x,y) coordinates is given by the known surface functions, z_1 and z_2, as: (see Fig. 1)

$$f(x,y) = z_2(x,y) - z_1(x,y) \qquad (2\text{-}1)$$

If the bodies are pressed together, points that are well removed from the contact region will undergo a rigid body motion, whereas points near the contact region will undergo a rigid body motion plus superposed elastic deformations. In general, the rigid-body motion of body 2 relative to body 1 is defined by six parameters. For simplicity, we assume, at this point, that the rigid body motion of body 2 relative to body 1 consists of a translation through distance δ in the negative direction of axis z. The quantity δ is called the rigid body approach. The methods of this paper may be extended to cover the more general case where several or all of the six possible degrees of (rigid-body) freedom are permitted.

Let us consider two points M_1 and M_2 on the surfaces of bodies 1 and 2 with common coordinates (x,y) as in Fig. 1. The initial separation vector between the two points will be:

$$\underset{\sim}{s}_i = f(x,y)\, \hat{\underset{\sim}{z}} \qquad (2\text{-}2)$$

where s_i is the initial separation between point M_1 and point M_2. $\hat{\underset{\sim}{z}}$ is the unit normal vector in the z-direction, and f(x,y) is given by Eq. (2-1). After deformation occurs, points M_1 and M_2 move to M_1' and M_2'.

If $\underset{\sim}{w}_1$ and $\underset{\sim}{w}_2$ represent the elastic displacement vectors of the points M_1 and M_2, then the final separation vector (i.e. separation vector after deformation), becomes (see Fig. 1)

$$\underset{\sim}{s}_f = \underset{\sim}{s}_i + \underset{\sim}{w}_2 - \underset{\sim}{w}_1 - \delta\, \hat{\underset{\sim}{z}} \qquad (2\text{-}3)$$

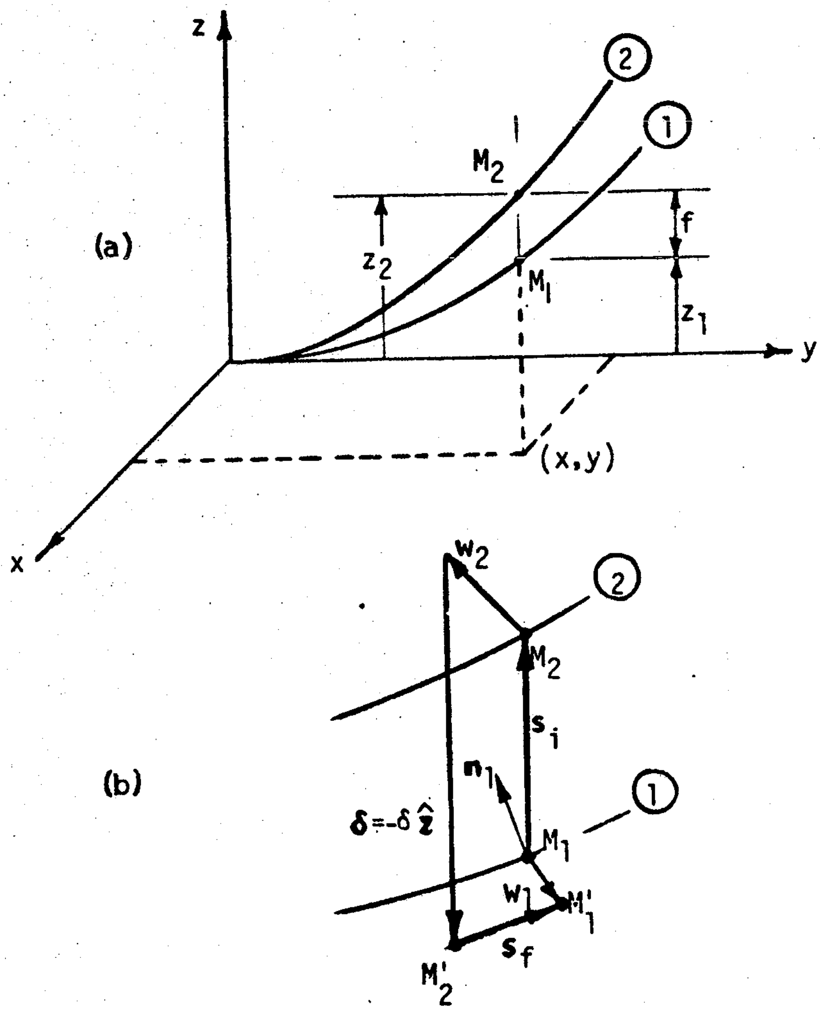

Fig. 1. The two bodies in contact under rigid body translation $\boldsymbol{\delta} = -\delta\hat{\mathbf{z}}$

(a) Curved lines are intersections of given surfaces with a plane through the z axis. The line M_1M_2 is parallel to the z-axis, prior to deformation.

(b) enlargement of region encircled in (a) showing the process of deformation

For closely conforming surfaces the normals to the two surfaces (at M_1 and M_2) differ very slightly in direction, and either of the two initial surfaces represents a good approximation to the deformed surface on which contact occurs. We will therefore assume that the contact patch lies on surface 1 (let body 1 be that of higher elastic modulus), and its unit normal vector $\underset{\sim}{n}$ will be approximated by $\underset{\sim}{n}_1$, the unit outward normal to surface 1.

Within the contact patch the component of separation $\underset{\sim}{s}_f$ in the normal direction vanishes, i.e. (see Fig. 1).

$$\underset{\sim}{s}_f \cdot \underset{\sim}{n} = (f\,\hat{\underset{\sim}{z}} + \underset{\sim}{w}_2 - \underset{\sim}{w}_1 - \delta\,\hat{\underset{\sim}{z}}) \cdot \underset{\sim}{n}_1 \approx 0 \qquad (2\text{-}4)$$

or

$$w_2^n + w_1^n = (\delta - f)\, n_z \text{ (within contact patch)} \qquad (2\text{-}5)$$

where

$$w_1^n = -\underset{\sim}{w}_1 \cdot \underset{\sim}{n}_1$$

$$w_2^n = -\underset{\sim}{w}_2 \cdot \underset{\sim}{n}_2 = \underset{\sim}{w}_2 \bullet \underset{\sim}{n}_1$$

are the components of $\underset{\sim}{w}_1$ and $\underset{\sim}{w}_2$ along the inward normals to surfaces 1 and 2; note that $\underset{\sim}{n}_1 \cong -\underset{\sim}{n}_2$, and n_z is the z-component of $\underset{\sim}{n}_1$.

The displacement w_i^n for body i is related to the pressure distribution over the contact region σ on body i by the expression

$$w_i(\underset{\sim}{r}) = \int_\sigma G_i(\underset{\sim}{r};\underset{\sim}{r}')\,p(\underset{\sim}{r}')\,d\sigma' \qquad (2\text{-}6)$$

where the so-called "Green's function" $G_i(\underset{\sim}{r};\underset{\sim}{r}')$ is the normal displacement of point $\underset{\sim}{r}$ due to a unit normal force on body i at $\underset{\sim}{r}'$.* Denoting the projection of area element $d\sigma'$ on the x-y plane by

$$dA' \equiv n_z'\, d\sigma' \qquad (2\text{-}7)$$

where n_z' is the z component of $\underset{\sim}{n}_i'$, we may write Eq.(2-6)in the form

$$w_i(\underset{\sim}{r}) = \int_\Omega G_i(\underset{\sim}{r};\underset{\sim}{r}')\,p(\underset{\sim}{r}')\,\frac{dA'}{n_z'} \qquad (2\text{-}8)$$

where Ω, the projection of σ on the x-y plane will henceforth be called the contact region.

---

*The tip of vector $\underset{\sim}{r}$ ($\underset{\sim}{r}'$) is called a field (source) point. Quantities evaluated at a source point will be marked by primes; e.g. $p'=p(\underset{\sim}{r}')$, but $p=p(\underset{\sim}{r})$.

Therefore equation (2-5) becomes

$$\int_{\Omega} (G_1 + G_2)p(\underset{\sim}{r}') \frac{dA'}{n_z'} = (\delta - f)\ n_z \qquad (2\text{-}9)$$

A physically meaningful solution requires that:

$$\begin{aligned} p(x,y) &> 0 \qquad \text{within } \Omega \\ p(x,y) &= 0 \qquad \text{on } C \end{aligned} \qquad (2\text{-}10)$$

where C is the boundary of the contact region Ω.

Equation (2-8) and condition (2-9) govern the conformal contact problem, and can be solved for p(x,y) and C, if a value of δ is specified.

The resultant force $\underset{\sim}{F}^{(p)}$ and moment $\underset{\sim}{M}^{(p)}$ (on body 1), may be found (see Figure 2) from the expressions

$$\underset{\sim}{F}^{(p)} = -\int_{\Omega} p\underset{\sim}{n}\ d\sigma \qquad (2\text{-}11)$$

$$\underset{\sim}{M}^{(p)} = -\int_{\Omega} \underset{\sim}{r} \times p\underset{\sim}{n}\ d\sigma \qquad (2\text{-}12)$$

where $\underset{\sim}{r} = (x,y,z)$, and $d\sigma = dA/n_z$ by Eq. (2-7). Thus the applied external force $\underset{\sim}{F} \equiv -\underset{\sim}{F}^{(p)}$ and moment $\underset{\sim}{M} = -\underset{\sim}{M}^{(p)}$ are given by

$$\{F_x, F_y, F_z\} = -\int_{\Omega} p\{n_x, n_y, n_z\} \frac{dA}{n_z} \qquad (2\text{-}13)$$

$$\begin{aligned} M_x &= \int_{\Omega} (y\ n_z - z\ n_y)\ p\ \frac{dA}{n_z} \\ M_y &= \int_{\Omega} (-x\ n_z + z\ n_x)\ p\ \frac{dA}{n_z} \\ M_z &= \int_{\Omega} (x\ n_y - y\ n_x)\ p\ \frac{dA}{n_z} \end{aligned} \qquad (2\text{-}14)$$

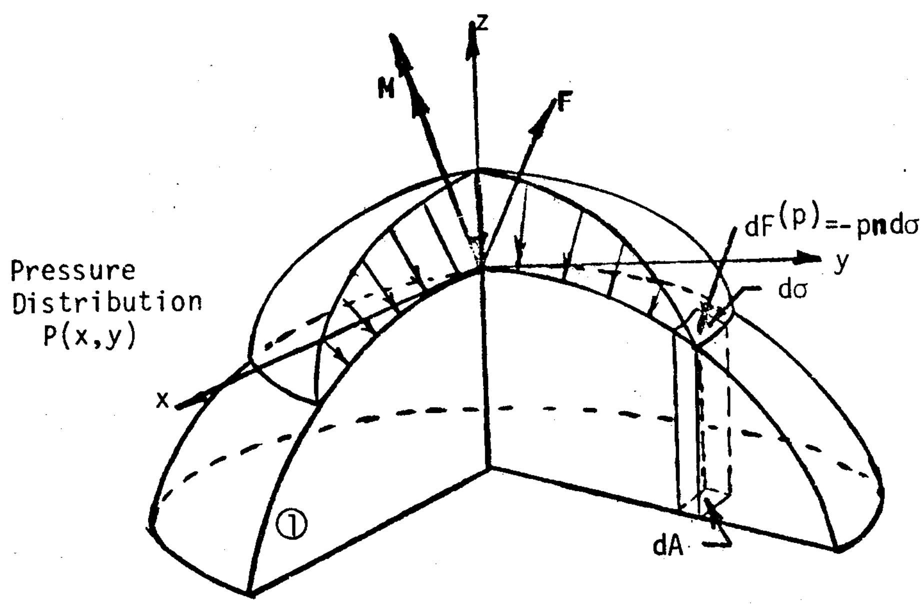

Fig. 2. Forces applied to body 1

3. DISCRETIZATION OF THE INTEGRAL EQUATION

For a given rigid body approach δ, Eq. (2-9) must be solved for the pressure field p(x,y) and for the contact region Ω . We will begin by assuming a candidate contact region Ω . The projection of the intersection curve which would arise if surface 1 were displaced relative to surface 2, along the z-axis by distance δ , on the x,y plane is called the interpenetration curve and is given by (see Fig. 3)

$$f(x,y) = z_2(x,y) - z_1(x,y) \qquad (3\text{-}1)$$

The region bounded by the interpenetration curve is chosen as the initial candidate contact region. Equation (2-9) becomes an integral equation of the first kind, which we will then solve by the modified simply discretized method*. Let us discretize the region Ω of the integral equation into n subregions $\Omega_1, \Omega_2, \ldots, \Omega_n$, where each subregion Ω_j is called "cell j". Then, Eq. (2-8) reduces to

$$\int_{\Omega_1}[G_1+G_2]\,\frac{p'dA'}{n_z'} + \int_{\Omega_2}[G_1+G_2]\,\frac{p'dA'}{n_z'} \;\ldots\ldots\; \int_{\Omega_n}[G_1+G_2]\,\frac{p'dA'}{n_z'} = [\delta-f(x,y)]n_z \qquad (3\text{-}2)$$

If cell j is small enough so that p(x',y') and $n_z(x',y')$ over that cell can be considered as constants p_j and n_z^j then Eq. (3-2) reduces to:

$$\int_{\Omega}(G_1+G_2)\,\frac{p'dA'}{n_z'} \approx \frac{p_1}{n_z^1}\int_{\Omega_1}(G_1+G_2)dA' + \frac{p_2}{n_z^2}\int_{\Omega_2}(G_1+G_2)dA' + \ldots + \frac{p_n}{n_z^n}\int_{\Omega_n}(G_1+G_2)dA'$$

$$\simeq[\delta-f(x,y)]\,n_z(x,y) \qquad (3\text{-}3)$$

The term (G_1+G_2) will be singular within certain cells and must therefore be kept under the integral sign, at least for such cells. In short,

$$\int_{\Omega}(G_1+G_2)\,\frac{p'dA'}{n_z'} \approx \sum_{j=1}^{n}\frac{p_j}{n_z^j}\int_{\Omega_j}(G_1+G_2)\,dA' \approx [\delta-f(x,y)]\,n_z(x,y) \qquad (3\text{-}4)$$

---

* Paul and Hashemi [1978-a]

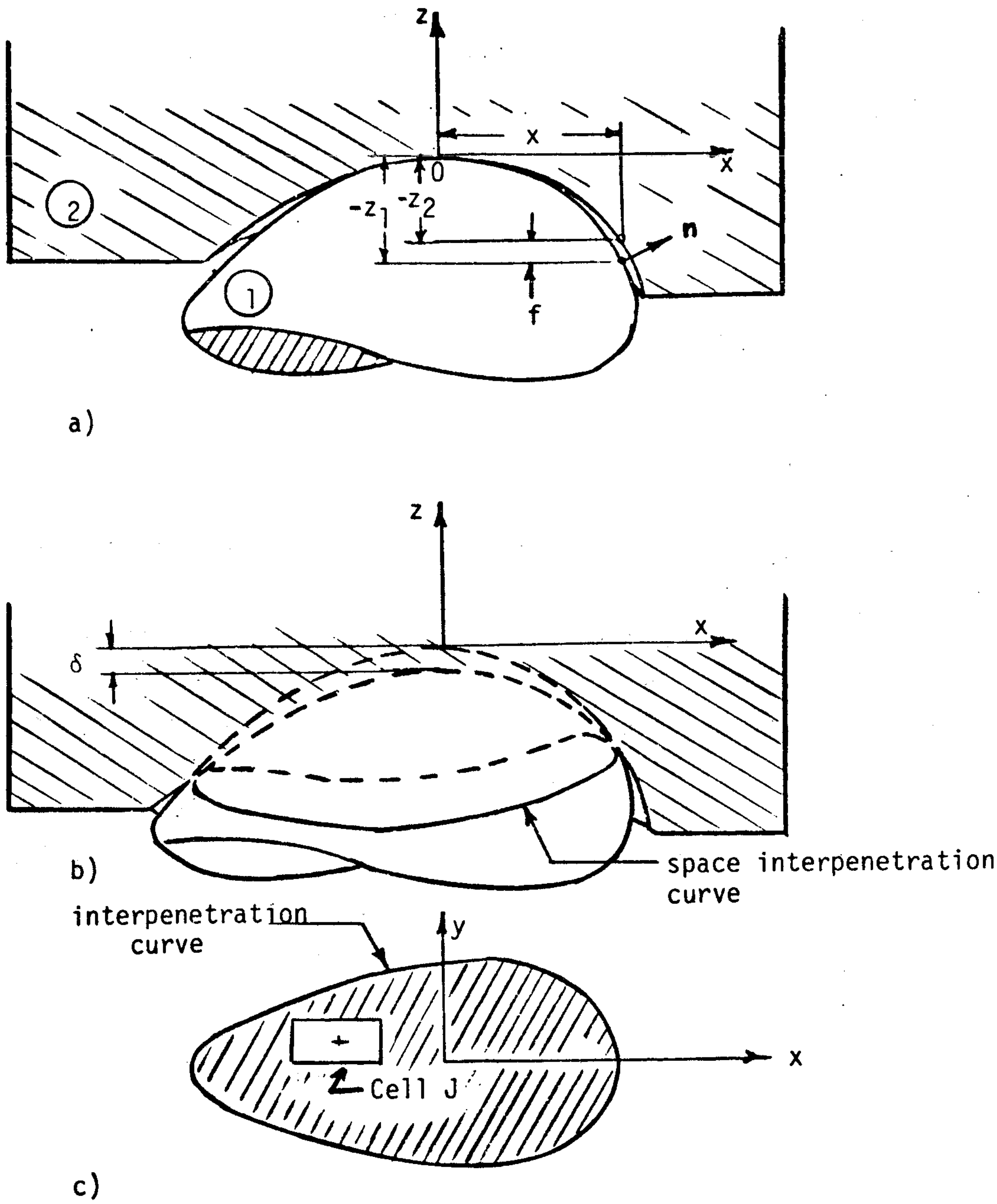

Fig 3. Two bodies in conformal contact
a) prior to deformation
b) ficticious interpenetration
c) initial candidate contact region

To find the unknown values of p_j we select n field points : (x_i, y_i) and write Eq. (3-4), for each of these points, in the form:

$$\sum_{j=1}^{n} b_{ij}\, p_j = d_i \qquad (i = 1,n) \tag{3-5}$$

where

$$b_{ij} = \frac{1}{n_z{}_j} \int_{\Omega_j} (G_1+G_2)\, dA' \tag{3-6}$$

$$d_i = [\delta - f(x_i, y_i)](n_z)_i \tag{3-7}$$

If matrix $[b_{ij}]$ is nonsingular, Eq. (3-5) may be solved for the candidate pressures p_j. If these values of p_j do not satisfy boundary conditions (2-9) we must modify the assumed contact region boundary C. The method used to choose and modify the boundary of Ω will be described in Sec. 5.

The Green's functions used for the specific examples of rail and wheel considered in this paper (sec. 7) are discussed in Appendix A. For further discussion on Green's functions see Hashemi and Paul [1979].

The applied force and moment are obtained from equations (2-13)and (2-14) as

$$F_x = \sum_{j=1}^{n} p_j \left(\frac{n_x}{n_z}\right)_j A_j \qquad\qquad M_x = \sum_{j=1}^{n} p_j \left[y - z\frac{n_y}{n_z}\right]_j A_j$$

$$F_y = \sum_{j=1}^{n} p_j \left(\frac{n_y}{n_z}\right)_j A_j \quad (3\text{-}8) \qquad\qquad M_y = \sum_{j=1}^{n} p_j \left[-x + z\frac{n_x}{n_z}\right]_j A_j \quad (3\text{-}9)$$

$$F_z = \sum_{j=1}^{n} p_j A_j \qquad\qquad M_z = \sum_{j=1}^{n} p_j [(x n_y - y n_x)/n_z]_j A_j$$

where A_j is area of cell j (in the x,y plane).

4. INITIAL CANDIDATE CONTACT BOUNDARY

The initial candidate contact region will be chosen as the region inside the "interpenetration curve," described in Sec. 3.

It was shown in Paul and Hashemi [1978-a] that for counterformal (but not necessarily Hertzian) contact, the actual contact region lies inside the interpenetration curve associated with a fixed approach. Similar reasoning shows that, in the case of conformal contact problems, the true contact patch lies inside the interpenetration curve, provided that the influence functions (Green's functions) used for both bodies are unidirectional,* over the initial candidate contact patch (see Hashemi [1979]). Experience to date suggests that the interpenetration curve is a good candidate for the initial contact patch, even for conformal contact.

5. MESH GENERATION AND CONTACT BOUNDARY DETERMINATION

The method devised by Paul and Hashemi [1978-a] for the mesh generation and boundary determination of counterformal problems has been improved and extended to the conformal problem . In the following, rectangular cells, with sides parallel to the x and y axis are utilized, and the contact region is assumed to be symmetric about the x-axis(as it would be for a wheel axis parallel to the x-axis, and a rail axis parallel to the y-axis); consequently, only half of the contact region (see Fig. 4) need be discussed. Both the field points and source points will be chosen to lie at the centroids of the rectangular cells. The scheme of subdivision for a candidate contact region is as follows:

Fig. 4 shows an example of such a region together with the coordinate axes (x,y). The x-diameter, which has known length a, may be divided into any number of segments (n_b) called Bands. A typical band (i) will be further divided into n_{si} number of segments called strips. That part of a strip which lies above the x-axis will be referred to as a half-strip. Then the "horizontal" length h_{xi} of cells in band i will be given by

$$h_{xi} = a_i/n_{si} \tag{5-1}$$

where

$$a_i = r_i a \tag{5-2}$$

and r_i is a fixed positive constant (less than 1) associated with band i, such

---

*An influence function will be described as unidirectional over a surface if a normal force applied to a point on the surface produces displacement at all points of the surface whose components in the direction of the applied force have the same sign everywhere.

that $\sum_i r_i = 1$

If we divide each half-strip j into a number of cells m_j, the "vertical" length h_y of each cell in that strip will be determined as:

$$h_{yj} = y_{max\ j}/m_j \tag{5-3a}$$

where $y_{max\ j}$ is the y-coordinate of the point on the boundary curve corresponding to the centerline of half-strip j (see Fig. 4).

If it is desired to have a field point on the x-axis, then we let

$$h_{yj} = y_{max\ j}/(m_j - \tfrac{1}{2}) \tag{5-3b}$$

The x-coordinate of the field points of all cells in the first strip will be obtained as:

$$x_1 = a_L + \frac{h_{x1}}{2} \tag{5.4}$$

where a_L is the left x-intercept of the boundary curve. Then the x-coordinate of the cell centroid in strip j > 1 becomes

$$x_j = x_{j-1} + h_{sj} \qquad (j > 1) \tag{5-5}$$

where $h_{sj} = h_{xi}$ and strip j is in band i.

Having unambiguously defined the cell arrangement, we may use Eqs. (3-6) and (3-7) to evaluate b_{ij} and d_i. Then the unknowns p_j may be found by solving the linear equations (3-5).

If the pressure distribution p_j does not satisfy conditions (2-10) the procedure explained in Paul and Hashemi [1978-a] will be used to redefine the new contact region boundary C. The whole process will be repeated until the conditions (2-10) are satisfied within a desired tolerance.

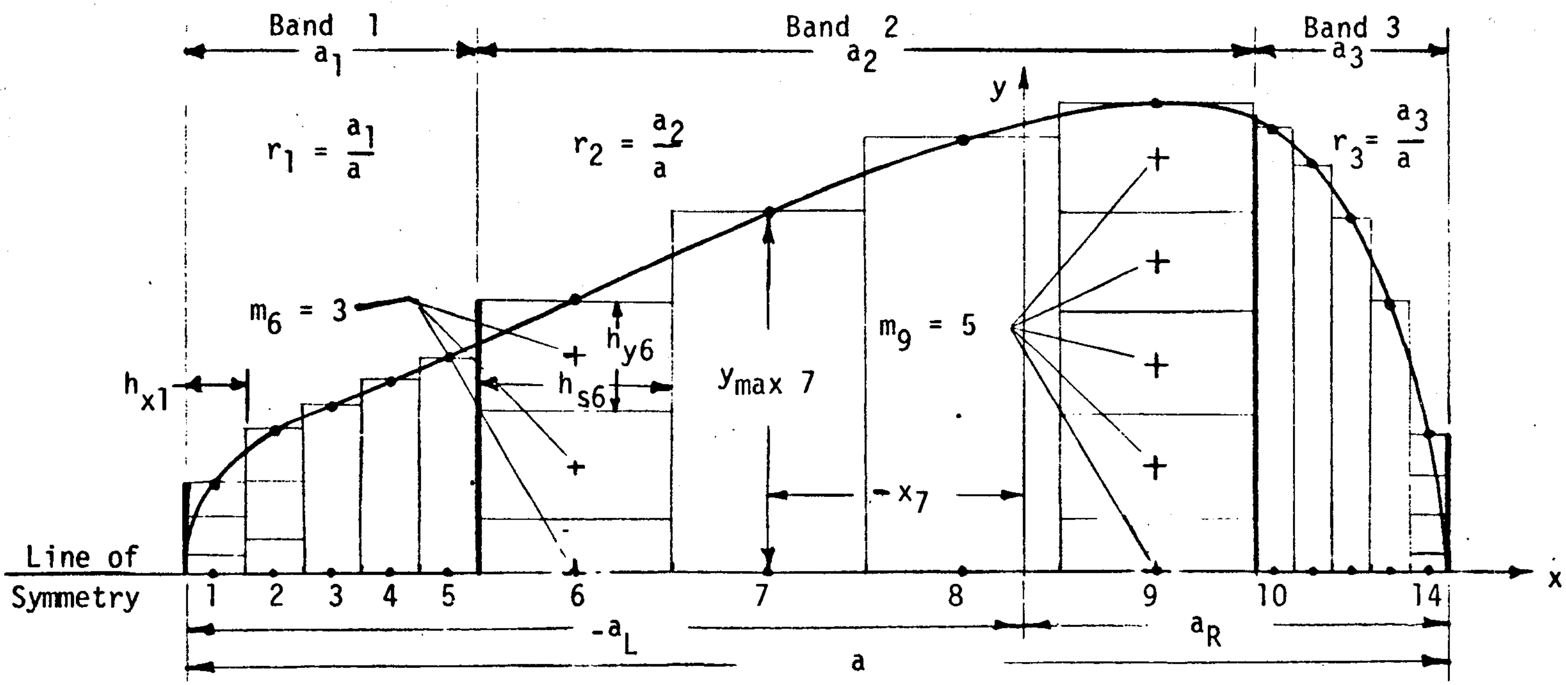

Fig. 4. Mesh arrangement for sample interpenetration curve. Bands are shown separated by heavy vertical lines. Band 1 is subdivided into 5 strips, band 2 into 4 strips, band 3 into 5 strips. Note that the x-axis is a line of symmetry, and only half of the contact patch is shown.

6. ORGANIZATION OF COMPUTER PROGRAM

The main program is called CONFORM which stands for "CONFORMal contact." The program is able to handle all contact problems with one axis of symmetry in its contact patch. In rail-wheel problems there will always be at least one axis of symmetry (parallel to the wheel axis) for wheel-sets at zero yaw angle.

MAIN PROGRAM--CONFORM*

The purpose of the main program is to manage input and output, to call appropriate subprograms as needed, and to interlink the various components needed for the overall program logic.

Figure 5 shows the relationship of the main program to the sub-programs. In Fig. 5, the arrows point from the calling program to the called program. The following subprograms are used:

Subfunction PARAB: does the parabolic interpolation (or extrapolation by a procedure referred to as PARAB2 in Paul and Hashemi [1978-a].

Subfunction BIF: calculates the integral $k \int dA/r$ of Boussinesq's function

Subfunction GDA: calculates $\int G\, dA$

Subfunction GR1: calculates $G(\underset{\sim}{r},\underset{\sim}{r}')$ for body (1) (Rail)**

Subfunction GR2: calculates $G(\underset{\sim}{r},\underset{\sim}{r}')$ for body (2) (Wheel)**

Subroutine LEQT1F: solves the linear algebraic equations (3-5).

Subroutine INSEP: furnishes the initial separaration; i.e. the profile function, Eq. (2-1), by a method described in Paul and Hashemi [1979].

Subroutine MIDWEL: provides the coordinates of an axial cross-section of a railroad wheel (body 2); i.e. it computes the term $z_2(x,0)$ of Eq. (2-1) in an appropriate set of coordinates (ζ,ξ) localized at the initial point of contact (see Fig. 6).

Subroutine WHEEL: computes the profile function $z_2(x,y)$ for body (2) (wheel) for any (x,y) in contact region.

Subroutine RAIL: computes the profile function $z_1(x,y)$ for body (1), the railhead.

---

*The program is described in greater depth in the User's manual [Paul and Hashemi, 1978-b].

**The Green's functions supplied with the program are described in Appendix A. Should the user wish to supply other types of Green's functions, he need only replace subroutines GR1 and GR2 with his own subroutines of the same name. A discussion of alternative choices of Green's functions is given in Hashemi and Paul [1979].

Subroutine WHEELO: calculates z_w and dz/dx of the wheel profile at any point with coordinate x_w in middle plane with respect to wheel reference coordinates $(x_w - z_w)$ fixed in an axial cross-section of the wheel.

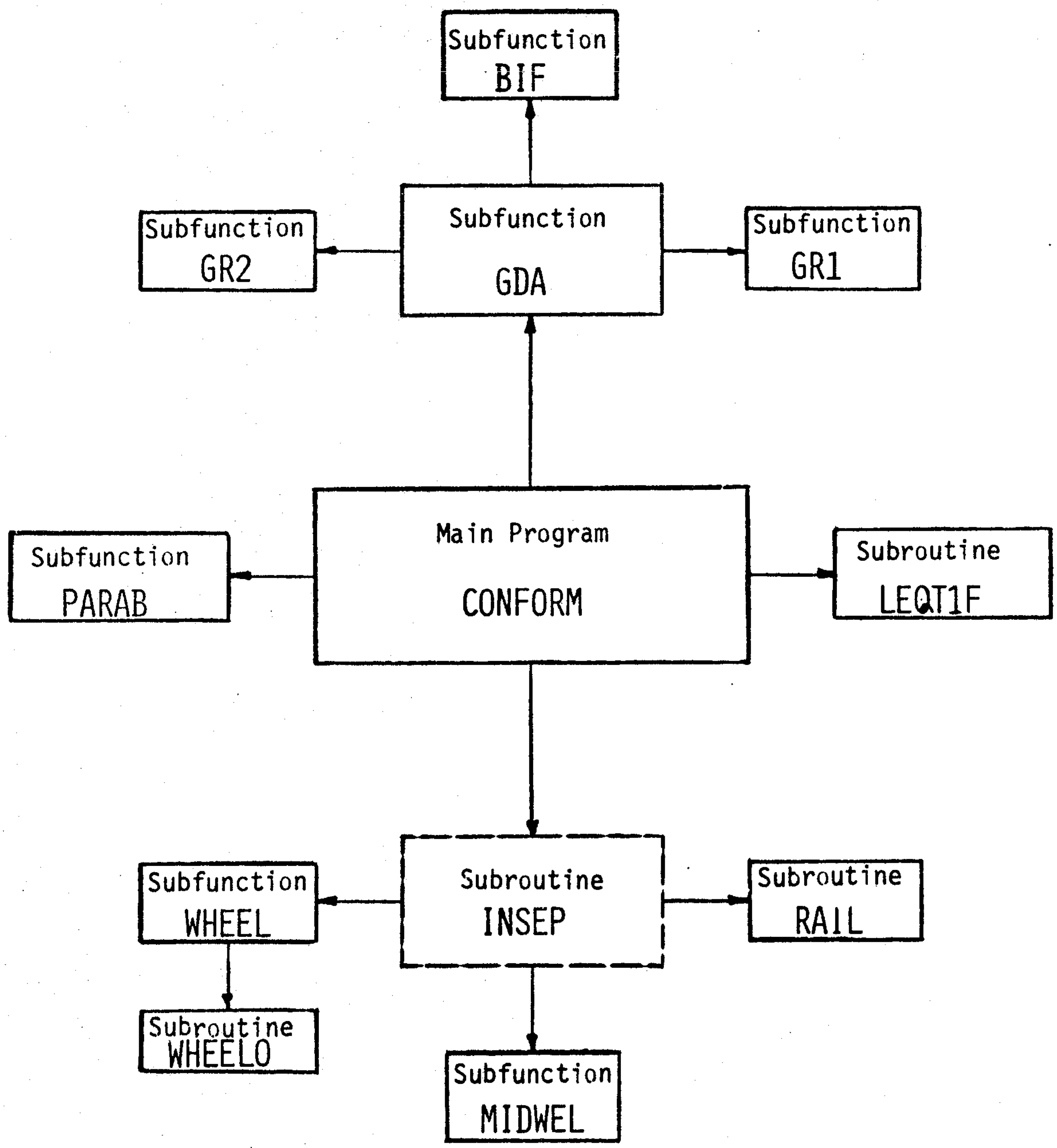

Fig. 5 Organization of Program CONFORM. Arrows point from calling program to called program
Dotted block may be user-supplied if user desires to override the standard subprograms provided.

7. EXAMPLES

The examples are given for rail and wheel contact where the wheel is so positioned that the problem could be either counterformal or conformal depending upon the magnitude of the applied load. In the first example, the applied load is relatively small so that the contact patch is counterformal, and the accuracy and reliability of the program CONFORM can be verified versus program COUNTACT* (see Fig. 7). In the second example the load is so high that the problem is highly conformal and the deviation between the two programs is significant (see Fig. 8).

The elastic properties of rail and wheel (steel) are

$E = 30 \times 10^6$ psi (Modulus of Elasticity)

$\nu = 0.3$ (Poisson's Ratio)

Example 1. COUNTERFORMAL CASE OF RAIL AND WHEEL CONTACT STRESSES

Let the initial point of contact of rail and wheel be point C shown in Fig. 6. For δ = 0.005" the numerical solution was found by using the computer program "COUNTACT-1" (counterformal contact stresses between bodies with one axis of symmetry in contact patch) and also by "CONFORM" (conformal contact stresses between two elastic bodies).

The program CONFORM requires, as part of the input, the rigid body approach δ , an initial candidate contact region, and the desired initial mesh arrangement. The final results are given in Table 1 for: pressure distribution, load (force and moment), and boundary of contact region.

A plot of pressure distribution along the ζ-axis is given in Fig. 7-a, and the contact region is shown in Fig. 7-b for both programs. Note that for the very light load applied (1413 lb), the contact patch is small and the problem is counterformal (but non-Hertzian). The excellent agreement between the predictions of programs COUNTACT and CONFORM, represents a validation of the latter program.

Example 2. CONFORMAL CASE OF RAIL AND WHEEL CONTACT STRESSES

For the same initial point of contact as in example 1, but for a higher load, the problem becomes conformal, and again the numerical solution of the problem was obtained by both CONFORM and COUNTACT , for δ = 0.003" (see Tables 2 and 3). The plot of pressure distribution along the ξ-axis is shown in Fig. 8-a. The contact patch is shown in Fig. 8-b.

*See Paul and Hashemi [1978-a].

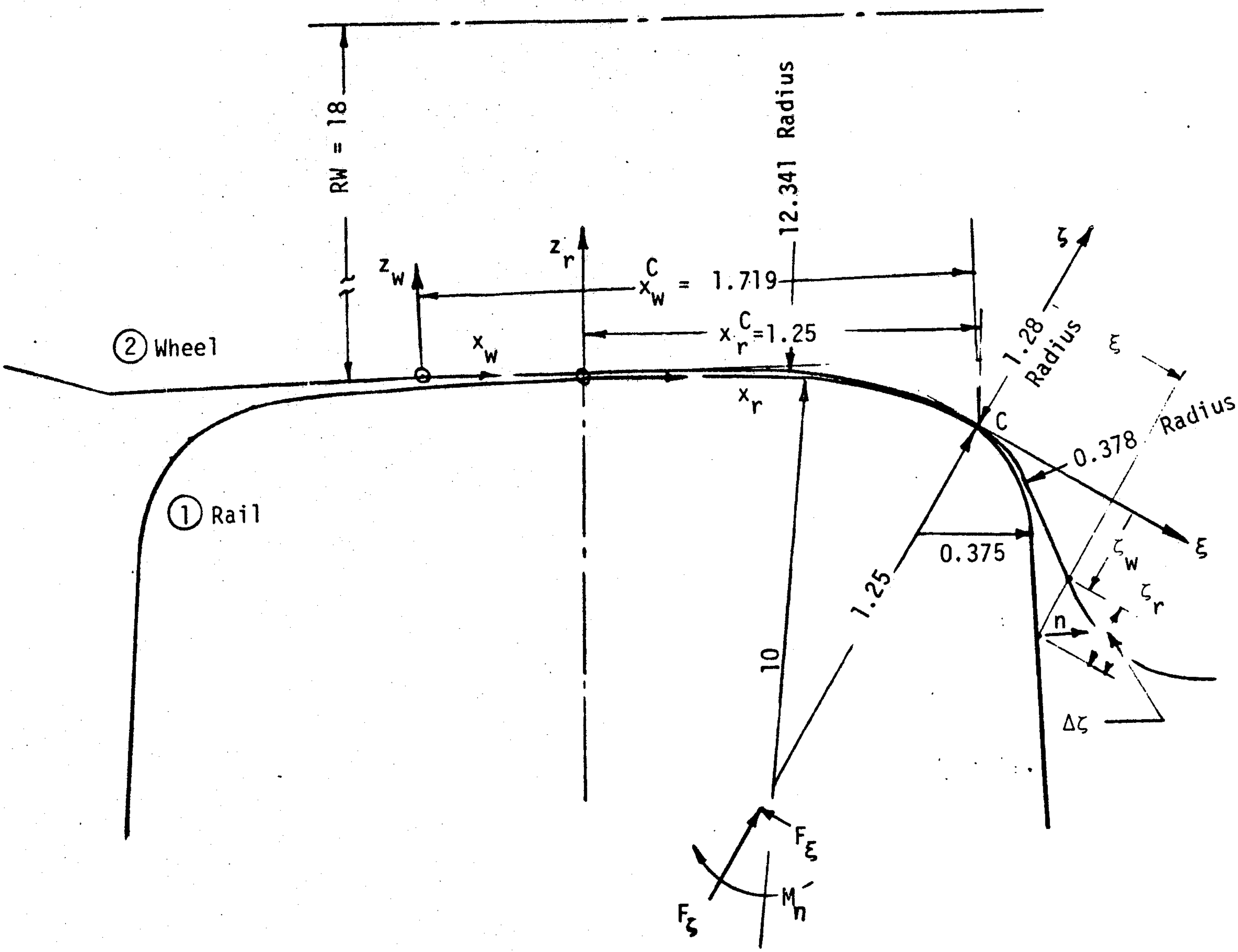

Fig. 6. Example of rail and wheel in conformal contact
(unloaded case shown)
Numerical data is for 140RE rail (AREA designation) and for SIG
Metroliner wheel (SIG=Schweitzerische Industrie-Gesellschaft)

Table 1. Contact boundary, pressure distribution, forces and moment (CONFORM), Example 1 (Normal force = 1413 lb)

BOUNDARY OF CONTACT REGION

XI	ETA	XI	ETA	XI	ETA
-0.1642115D 00	0.2901412D-01	-0.1484547D 00	0.4676656D-01	-0.1326978D 00	0.5881615D-01
-0.1169409D 00	0.6646521D-01	-0.9015417D-01	0.6122698D-01	-0.5233765D-01	0.9227063D-01
-0.1452112D-01	0.9711553D-01	0.2329541D-01	0.1003011D 00	0.6111193D-01	0.9848131D-01
0.8789864D-01	0.8672366D-01	0.1036555D 00	0.6053525D-01	0.1194124D 00	0.6804475D-01
0.1351693D 00	0.4485440D-01				

NODE	XI	ETA	ZETA	P
1	-0.1642D 00	0.0000D 00	-0.1083D-01	0.1269D 05
2	-0.1642D 00	0.1161D-01	-0.1083D-01	0.1189D 05
3	-0.1642D 00	0.2321D-01	-0.1083D-01	0.7180D 04
4	-0.1485D 00	0.0000D 00	-0.8847D-02	0.2241D 05
5	-0.1485D 00	0.1871D-01	-0.8847D-02	0.2089D 05
6	-0.1485D 00	0.3741D-01	-0.8847D-02	0.1296D 05
7	-0.1327D 00	0.0000D 00	-0.7063D-02	0.2691D 05
8	-0.1327D 00	0.1681D-01	-0.7063D-02	0.2625D 05
9	-0.1327D 00	0.3361D-01	-0.7063D-02	0.2242D 05
10	-0.1327D 00	0.5042D-01	-0.7063D-02	0.1294D 05
11	-0.1169D 00	0.0000D 00	-0.5482D-02	0.3090D 05
12	-0.1169D 00	0.1477D-01	-0.5482D-02	0.3050D 05
13	-0.1169D 00	0.2954D-01	-0.5482D-02	0.2800D 05
14	-0.1169D 00	0.4431D-01	-0.5482D-02	0.2346D 05
15	-0.1169D 00	0.5908D-01	-0.5482D-02	0.1376D 05
16	-0.9015D-01	0.0000D 00	-0.3255D-02	0.3606D 05
17	-0.9015D-01	0.3249D-01	-0.3255D-02	0.3315D 05
18	-0.9015D-01	0.6498D-01	-0.3255D-02	0.1871D 05
19	-0.5234D-01	0.0000D 00	-0.1096D-02	0.4030D 05
20	-0.5234D-01	0.3691D-01	-0.1096D-02	0.3707D 05
21	-0.5234D-01	0.7382D-01	-0.1096D-02	0.2056D 05
22	-0.1452D-01	0.0000D 00	-0.8435D-04	0.4232D 05
23	-0.1452D-01	0.3885D-01	-0.8435D-04	0.3884D 05
24	-0.1452D-01	0.7769D-01	-0.8435D-04	0.2171D 05
25	0.2330D-01	0.0000D 00	-0.7243D-03	0.4227D 05
26	0.2330D-01	0.4012D-01	-0.7243D-03	0.3888D 05
27	0.2330D-01	0.8024D-01	-0.7243D-03	0.2173D 05
28	0.6111D-01	0.0000D 00	-0.5013D-02	0.3831D 05
29	0.6111D-01	0.3939D-01	-0.5013D-02	0.3525D 05
30	0.6111D-01	0.7879D-01	-0.5013D-02	0.1991D 05
31	0.8790D-01	0.0000D 00	-0.1045D-01	0.3294D 05
32	0.8790D-01	0.1927D-01	-0.1045D-01	0.3303D 05
33	0.8790D-01	0.3854D-01	-0.1045D-01	0.2979D 05
34	0.8790D-01	0.5782D-01	-0.1045D-01	0.2597D 05
35	0.8790D-01	0.7709D-01	-0.1045D-01	0.1516D 05
36	0.1037D 00	0.0000D 00	-0.1461D-01	0.2854D 05
37	0.1037D 00	0.1790D-01	-0.1461D-01	0.2842D 05
38	0.1037D 00	0.3579D-01	-0.1461D-01	0.2613D 05
39	0.1037D 00	0.5369D-01	-0.1461D-01	0.2193D 05
40	0.1037D 00	0.7159D-01	-0.1461D-01	0.1273D 05
41	0.1194D 00	0.0000D 00	-0.1952D-01	0.2355D 05
42	0.1194D 00	0.1512D-01	-0.1952D-01	0.2341D 05
43	0.1194D 00	0.3024D-01	-0.1952D-01	0.2164D 05
44	0.1194D 00	0.4536D-01	-0.1952D-01	0.1810D 05
45	0.1194D 00	0.6048D-01	-0.1952D-01	0.1047D 05
46	0.1352D 00	0.0000D 00	-0.2521D-01	0.1349D 05
47	0.1352D 00	0.1794D-01	-0.2521D-01	0.1249D 05
48	0.1352D 00	0.3588D-01	-0.2521D-01	0.7595D 04

XI-FORCE= 68.1 ETA-FORCE= 1413.1 ETA-MOMENT= -7.5

LEFT XI-BOUNDARY= -0.17165 RIGHT XI-BOUNDARY= 0.14286

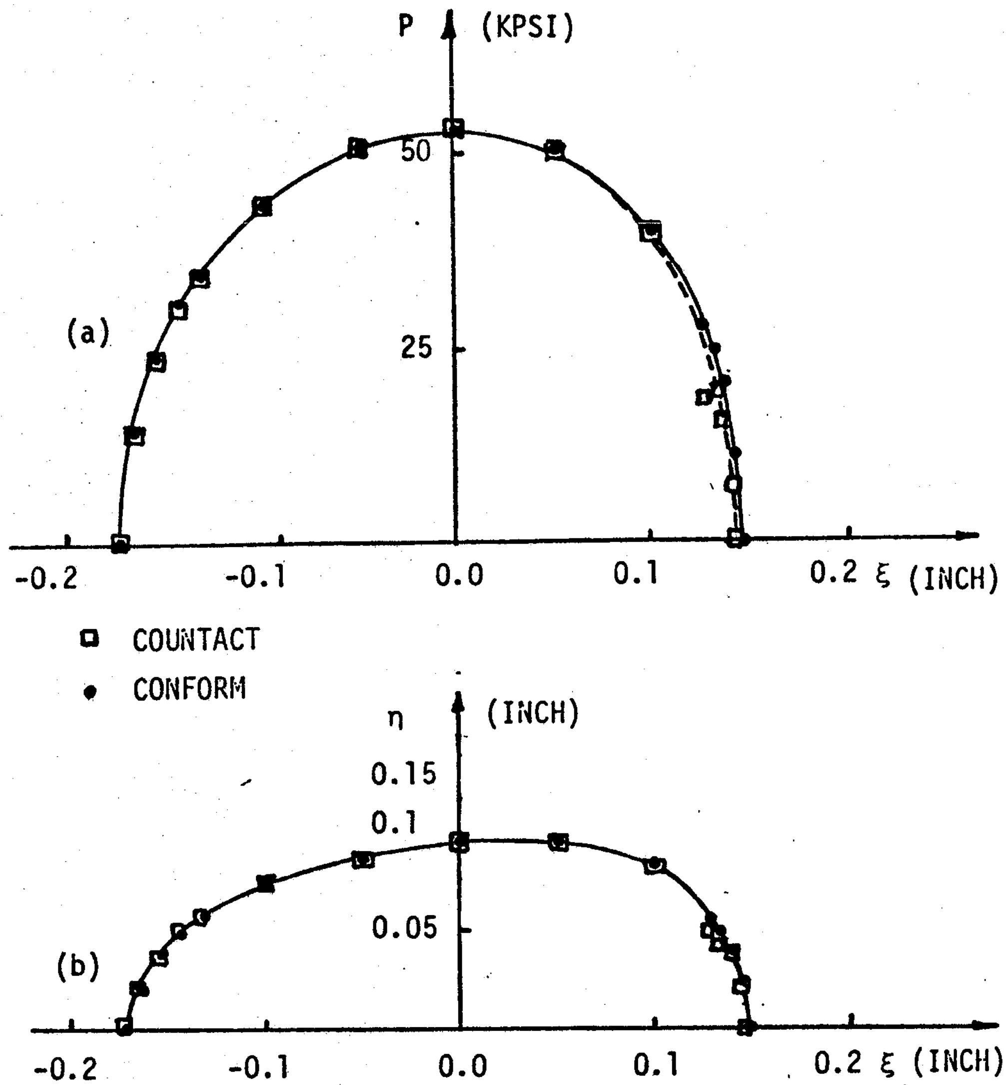

Fig. 7. Comparison of Programs CONFORM and COUNTACT for $\delta = 0.0005$." The corresponding forces are: F = 1413 lb (CONFORM), F = 1434 lb (COUNTACT)
(a) Pressure distribution
(b) Contact patch

Table 2. Contact boundary, pressure distribution, forces and moment, solved by program <u>CONFORM</u>.

BOUNDARY OF CONTACT REGION

XI	ETA	XI	ETA	XI	ETA
-0.3591756D 00	0.9918354D-01	-0.2755054D 00	0.1582061D 00	-0.1918351D 00	0.1937786D 00
-0.1000000D 00	0.2188504D 00	0.0000000D 00	0.2329395D 00	0.1000000D 00	0.2597492D 00
0.1571789D 00	0.2663273D 00	0.1715366D 00	0.2654181D 00	0.1858944D 00	0.2605813D 00
0.2002521D 00	0.2572054D 00	0.2146099D 00	0.2476021D 00	0.2289676D 00	0.1909905D 00

NODE	XI	ETA	ZETA	P
1	-0.3592D 00	0.0000D 00	-0.5271D-01	0.4703D 05
2	-0.3592D 00	0.2204D-01	-0.5271D-01	0.4554D 05
3	-0.3592D 00	0.4408D-01	-0.5271D-01	0.4156D 05
4	-0.3592D 00	0.6612D-01	-0.5271D-01	0.3434D 05
5	-0.3592D 00	0.8816D-01	-0.5271D-01	0.2120D 05
6	-0.2755D 00	0.0000D 00	-0.3074D-01	0.7980D 05
7	-0.2755D 00	0.3516D-01	-0.3074D-01	0.7800D 05
8	-0.2755D 00	0.7031D-01	-0.3074D-01	0.7214D 05
9	-0.2755D 00	0.1055D 00	-0.3074D-01	0.6058D 05
10	-0.2755D 00	0.1406D 00	-0.3074D-01	0.3702D 05
11	-0.1918D 00	0.0000D 00	-0.1481D-01	0.9453D 05
12	-0.1918D 00	0.4306D-01	-0.1481D-01	0.9226D 05
13	-0.1918D 00	0.8612D-01	-0.1481D-01	0.8509D 05
14	-0.1918D 00	0.1292D 00	-0.1481D-01	0.7180D 05
15	-0.1918D 00	0.1722D 00	-0.1481D-01	0.4395D 05
16	-0.1000D 00	0.0000D 00	-0.4006D-02	0.1037D 06
17	-0.1000D 00	0.4863D-01	-0.4006D-02	0.1014D 06
18	-0.1000D 00	0.9727D-01	-0.4006D-02	0.9335D 05
19	-0.1000D 00	0.1459D 00	-0.4006D-02	0.7867D 05
20	-0.1000D 00	0.1945D 00	-0.4006D-02	0.4811D 05
21	0.0000D 00	0.0000D 00	0.0000D 00	0.1104D 06
22	0.0000D 00	0.5176D-01	0.0000D 00	0.1076D 06
23	0.0000D 00	0.1035D 00	0.0000D 00	0.9841D 05
24	0.0000D 00	0.1553D 00	0.0000D 00	0.8181D 05
25	0.0000D 00	0.2071D 00	0.0000D 00	0.4919D 05
26	0.1000D 00	0.0000D 00	-0.1358D-01	0.1027D 06
27	0.1000D 00	0.5772D-01	-0.1358D-01	0.1001D 06
28	0.1000D 00	0.1154D 00	-0.1358D-01	0.9231D 05
29	0.1000D 00	0.1732D 00	-0.1358D-01	0.7749D 05
30	0.1000D 00	0.2309D 00	-0.1358D-01	0.4659D 05
31	0.1572D 00	0.0000D 00	-0.3453D-01	0.8483D 05
32	0.1572D 00	0.5918D-01	-0.3453D-01	0.8275D 05
33	0.1572D 00	0.1184D 00	-0.3453D-01	0.7605D 05
34	0.1572D 00	0.1776D 00	-0.3453D-01	0.6412D 05
35	0.1572D 00	0.2367D 00	-0.3453D-01	0.3919D 05
36	0.1715D 00	0.0000D 00	-0.4153D-01	0.7848D 05
37	0.1715D 00	0.5898D-01	-0.4153D-01	0.7654D 05
38	0.1715D 00	0.1180D 00	-0.4153D-01	0.7041D 05
39	0.1715D 00	0.1769D 00	-0.4153D-01	0.5929D 05
40	0.1715D 00	0.2359D 00	-0.4153D-01	0.3540D 05
41	0.1859D 00	0.0000D 00	-0.4932D-01	0.7090D 05
42	0.1859D 00	0.5791D-01	-0.4932D-01	0.6913D 05
43	0.1859D 00	0.1158D 00	-0.4932D-01	0.6381D 05
44	0.1859D 00	0.1737D 00	-0.4932D-01	0.5404D 05
45	0.1859D 00	0.2316D 00	-0.4932D-01	0.3378D 05
46	0.2003D 00	0.0000D 00	-0.5794D-01	0.6298D 05
47	0.2003D 00	0.5716D-01	-0.5794D-01	0.6159D 05
48	0.2003D 00	0.1143D 00	-0.5794D-01	0.5656D 05
49	0.2003D 00	0.1715D 00	-0.5794D-01	0.4743D 05
50	0.2003D 00	0.2286D 00	-0.5794D-01	0.2812D 05
51	0.2146D 00	0.0000D 00	-0.6748D-01	0.5173D 05
52	0.2146D 00	0.5502D-01	-0.6748D-01	0.4991D 05
53	0.2146D 00	0.1100D 00	-0.6748D-01	0.4626D 05
54	0.2146D 00	0.1651D 00	-0.6748D-01	0.3935D 05
55	0.2146D 00	0.2201D 00	-0.6748D-01	0.2542D 05
56	0.2290D 00	0.0000D 00	-0.7802D-01	0.3924D 05
57	0.2290D 00	0.4244D-01	-0.7802D-01	0.3987D 05
58	0.2290D 00	0.8488D-01	-0.7802D-01	0.3716D 05
59	0.2290D 00	0.1273D 00	-0.7802D-01	0.3125D 05
60	0.2290D 00	0.1698D 00	-0.7802D-01	0.2282D 05

XI-FORCE=1244.345 ZETA-FORCE =18965.182 ETA-MOMENT= 2158.806

LEFT XI-BOUNDARY=-0.4036896 RIGHT XI-BOUNDARY= 0.2484127

Table 3. Contact boundary, pressure distribution, forces and moment, Example 2, solved by program COUNTACT

BOUNDARY OF CONTACT REGION

XI	ETA	XI	ETA	XI	ETA
-0.3782336D 00	0.8182235D-01	-0.3223402D 00	0.1330270D 00	-0.2664467D 00	0.1663680D 00
-0.2120000D 00	0.1869911D 00	-0.1590000D 00	0.2048687D 00	-0.1060000D 00	0.2169514D 00
-0.5300000D-01	0.2255931D 00	0.0000000D 00	0.2276853D 00	0.5300000D-01	0.2455255D 00
0.1060000D 00	0.2586600D 00	0.1590000D 00	0.2718343D 00	0.2120000D 00	0.2783544D 00
0.2387366D 00	0.2351866D 00	0.2392158D 00	0.1872592D 00	0.2396930D 00	0.1603641D 00
0.2401701D 00	0.8767804D-01				

NODE	XI	ETA	ZETA	P
1	-0.3782D 00	0.0000D 00	-0.5860D-01	0.4094D 05
2	-0.3782D 00	0.1818D-01	-0.5860D-01	0.3951D 05
3	-0.3782D 00	0.3637D-01	-0.5860D-01	0.3574D 05
4	-0.3782D 00	0.5455D-01	-0.5860D-01	0.2915D 05
5	-0.3782D 00	0.7273D-01	-0.5860D-01	0.1705D 05
6	-0.3223D 00	0.0000D 00	-0.4228D-01	0.7073D 05
7	-0.3223D 00	0.2956D-01	-0.4228D-01	0.6902D 05
8	-0.3223D 00	0.5912D-01	-0.4228D-01	0.6365D 05
9	-0.3223D 00	0.8868D-01	-0.4228D-01	0.5280D 05
10	-0.3223D 00	0.1182D 00	-0.4228D-01	0.2980D 05
11	-0.2664D 00	0.0000D 00	-0.2873D-01	0.8456D 05
12	-0.2664D 00	0.3697D-01	-0.2873D-01	0.8245D 05
13	-0.2664D 00	0.7394D-01	-0.2873D-01	0.7589D 05
14	-0.2664D 00	0.1109D 00	-0.2873D-01	0.6354D 05
15	-0.2664D 00	0.1479D 00	-0.2873D-01	0.3584D 05
16	-0.2120D 00	0.0000D 00	-0.1811D-01	0.9319D 05
17	-0.2120D 00	0.4200D-01	-0.1811D-01	0.9090D 05
18	-0.2120D 00	0.8400D-01	-0.1811D-01	0.8362D 05
19	-0.2120D 00	0.1260D 00	-0.1811D-01	0.7005D 05
20	-0.2120D 00	0.1680D 00	-0.1811D-01	0.4004D 05
21	-0.1590D 00	0.0000D 00	-0.1015D-01	0.9847D 05
22	-0.1590D 00	0.4553D-01	-0.1015D-01	0.9606D 05
23	-0.1590D 00	0.9105D-01	-0.1015D-01	0.8838D 05
24	-0.1590D 00	0.1366D 00	-0.1015D-01	0.7413D 05
25	-0.1590D 00	0.1821D 00	-0.1015D-01	0.4323D 05
26	-0.1060D 00	0.0000D 00	-0.4503D-02	0.1016D 06
27	-0.1060D 00	0.4821D-01	-0.4503D-02	0.9915D 05
28	-0.1060D 00	0.9642D-01	-0.4503D-02	0.9123D 05
29	-0.1060D 00	0.1446D 00	-0.4503D-02	0.7654D 05
30	-0.1060D 00	0.1928D 00	-0.4503D-02	0.4505D 05
31	-0.5300D-01	0.0000D 00	-0.1124D-02	0.1032D 06
32	-0.5300D-01	0.5013D-01	-0.1124D-02	0.1006D 06
33	-0.5300D-01	0.1003D 00	-0.1124D-02	0.9248D 05
34	-0.5300D-01	0.1504D 00	-0.1124D-02	0.7754D 05
35	-0.5300D-01	0.2005D 00	-0.1124D-02	0.4571D 05
36	0.0000D 00	0.0000D 00	0.0000D 00	0.1036D 06
37	0.0000D 00	0.5060D-01	0.0000D 00	0.1007D 06
38	0.0000D 00	0.1012D 00	0.0000D 00	0.9224D 05
39	0.0000D 00	0.1518D 00	0.0000D 00	0.7598D 05
40	0.0000D 00	0.2024D 00	0.0000D 00	0.4445D 05
41	0.5300D-01	0.0000D 00	-0.3764D-02	0.1031D 06
42	0.5300D-01	0.5456D-01	-0.3764D-02	0.1005D 06
43	0.5300D-01	0.1091D 00	-0.3764D-02	0.9216D 05
44	0.5300D-01	0.1637D 00	-0.3764D-02	0.7743D 05
45	0.5300D-01	0.2182D 00	-0.3764D-02	0.4507D 05
46	0.1060D 00	0.0000D 00	-0.1529D-01	0.1030D 06
47	0.1060D 00	0.5748D-01	-0.1529D-01	0.1004D 06
48	0.1060D 00	0.1150D 00	-0.1529D-01	0.9209D 05
49	0.1060D 00	0.1724D 00	-0.1529D-01	0.7717D 05
50	0.1060D 00	0.2299D 00	-0.1529D-01	0.4529D 05
51	0.1590D 00	0.0000D 00	-0.3538D-01	0.1053D 06
52	0.1590D 00	0.6041D-01	-0.3538D-01	0.1026D 06
53	0.1590D 00	0.1208D 00	-0.3538D-01	0.9414D 05
54	0.1590D 00	0.1812D 00	-0.3538D-01	0.7852D 05
55	0.1590D 00	0.2416D 00	-0.3538D-01	0.4564D 05
56	0.2120D 00	0.0000D 00	-0.6568D-01	0.9785D 05
57	0.2120D 00	0.6186D-01	-0.6568D-01	0.9538D 05
58	0.2120D 00	0.1237D 00	-0.6568D-01	0.8774D 05
59	0.2120D 00	0.1856D 00	-0.6568D-01	0.7322D 05
60	0.2120D 00	0.2474D 00	-0.6568D-01	0.4256D 05
61	0.2387D 00	0.0000D 00	-0.8581D-01	0.7401D 06
62	0.2387D 00	0.5226D-01	-0.8581D-01	0.6589D 06
63	0.2387D 00	0.1045D 00	-0.8581D-01	0.6561D 06
64	0.2387D 00	0.1568D 00	-0.8581D-01	0.6862D 06
65	0.2387D 00	0.2091D 00	-0.8581D-01	0.4615D 06
66	0.2392D 00	0.0000D 00	-0.8621D-01	0.3319D 06
67	0.2392D 00	0.4161D-01	-0.8621D-01	0.4000D 06
68	0.2392D 00	0.8323D-01	-0.8621D-01	0.4425D 06
69	0.2392D 00	0.1248D 00	-0.8621D-01	0.2550D 06
70	0.2392D 00	0.1665D 00	-0.8621D-01	0.1432D 06
71	0.2397D 00	0.0000D 00	-0.8660D-01	0.2186D 06
72	0.2397D 00	0.3564D-01	-0.8660D-01	0.2582D 06
73	0.2397D 00	0.7127D-01	-0.8660D-01	0.1575D 06
74	0.2397D 00	0.1069D 00	-0.8660D-01	0.1914D 06
75	0.2397D 00	0.1425D 00	-0.8660D-01	0.1332D 06
76	0.2402D 00	0.0000D 00	-0.8700D-01	0.1101D 06
77	0.2402D 00	0.1948D-01	-0.8700D-01	0.6213D 05
78	0.2402D 00	0.3897D-01	-0.8700D-01	0.1447D 06
79	0.2402D 00	0.5845D-01	-0.8700D-01	0.8357D 05
80	0.2402D 00	0.7794D-01	-0.8700D-01	0.2940D 05

XI-FORCE =2541.523 ZETA-FORCE= 20552.141 ETA- MOMENT= 2022.316

LEFT XI-BOUNDARY=-0.4064102 RIGHT XI-BOUNDARY= 0.2403322

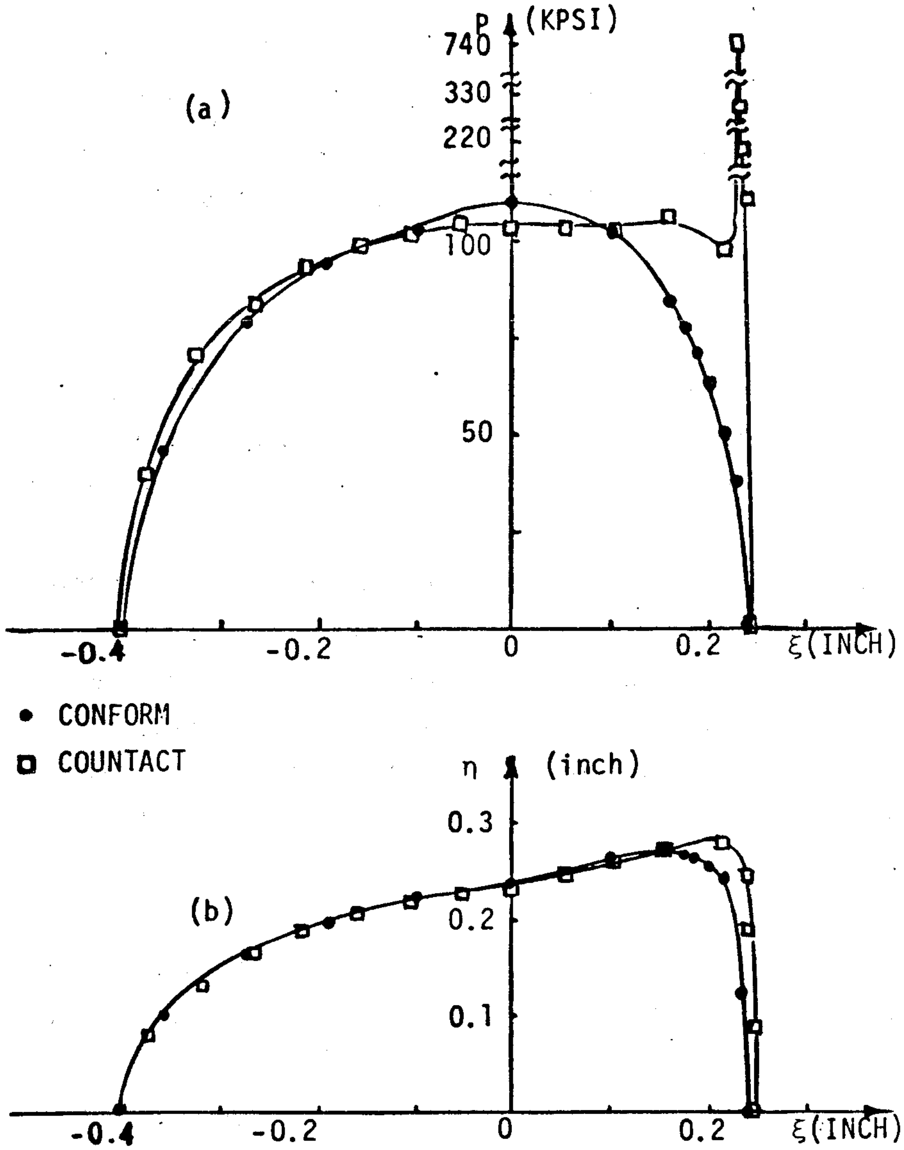

Fig. 8 Comparison of Programs CONFORM and COUNTACT for δ = 0.003"
F = 20550 lb (COUNTACT), F = 19000 lb (CONFORM)
(a) Pressure distribution along the ξ axis
(b) Contact patch

Note that the contact boundary predicted by COUNTACT is not too different from that predicted by CONFORM. However, COUNTACT predicts a very extreme pressure concentration (740,000 psi), whereas the more accurate program CONFORM shows that the peak pressure is actually 110,400 psi.

8. CONCLUSIONS

The modified simply discretized method of Paul and Hashemi [1978-a] has been extended to conformal problems. Methods for automatic mesh generation and contact patch boundary determination have also been extended to conformal contact problems.

Computer program CONFORM, based on these ideas, has been described and numerical results were presented for selected examples.

The first numerical example demonstrates the accuracy of program CONFORM for the special case of non-Hertzian counterformal contact problems. The accuracy of program CONFORM for this class of problems checked against the more specialized program COUNTACT, which is limited to strictly counterformal problems. Figure 7 illustrates the validity of program CONFORM for this verifiable case.

The second example presents the first known solution to the conformal contact stress problem for geometry as complex as that of a realistic rail-head and wheel making contact on the throat of the flange.

Figure 8-a illustrates how important it is to use program CONFORM for truly conformal cases, and that practical cases of conformal problems occur, which cannot be adequately approximated by a procedure designed for counterformal cases.

REFERENCES

Hashemi, J. and Paul, B., "Contact Stresses on Bodies with Arbitrary Geometry, Applications to Wheels and Rails," Report No. FRA-ORD-79/23, Technical Report No. 7, April 1979, Also see Ph.D. dissertation of J. Hashemi, University of Pennsylvania (1979).

Lur'e, A. I., Three Dimensional Problems of the Theory of Elasticity, Interscience, N.Y. (1964).

Paul, B. and Hashemi, J., "User's Manual for Program COUNTACT (COUNTerformal contACT stress problems)", Technical Report No. 4, September 1977, FRA-ORD-78-27, Contract DOT-OS-60144, Federal Railroad Administration. Also MEAM Report 77-2, Department of Mechanical Engineering and Applied Mechanics, University of Pennsylvania, Philadelphia (1977).

Paul, B., and Hashemi, J., "An Improved Numerical Method and Computer Program for Counterformal Contact Stress Problems," ASME, Computational Techniques for Interfact Problems, AMD-Vol. 30 (1978). Also Report No. FRA-ORD-78/26, Federal Railroad Administration, Technical Report No. 3, July 1977,and MEAM Report No. 77-1, University of Pennsylvania, Philadelphia, (1978-a).

Paul, B., and Hashemi, J., "User's Manual for Program CONFORM (CONFORMal contact stress problems)", Technical Report No. 5, June 1978, FRA/ORD-78/40, Contract No. DOT-OS-60144, Federal Railroad Administration. Also MEAM Report 78-1, Department of Mechanical Engineering and Applied Mechanics, University of Pennsylvania, Philadelphia, (1978-b).

Paul, B., and Hashemi, J., "Wheel-Rail Geometry Associated with Contact Stress Analysis," Technical Report No. 6, To be issued (1979).

Singh, K. P., and Paul, B., "Numerical Solution of Non-Hertzian Elastic Contact Problems", Journal of Applied Mechanics, Transactions of ASME, pp. 29-35 (1974).

Woodward, W., and Paul, B., "Contact Stresses for Closely Conforming Bodies - Application to Cylinders and Spheres", Technical Report No. 2, December 1976, DOT-TST-77-48, PB271033, Contract DOT-OS-40093(1976).

APPENDIX A: Influence Function for Rail and Wheel Surfaces

One of the major difficulties in the solution of any contact problem is the determination of suitable Green's functions for the surfaces in contact. These "influence functions" relate the elastic displacement at a given point due to a unit applied force at some other point. In contact problems, we are concerned with the elastic displacements of surface points due to a unit load applied anywhere on the surface of a body.

In counterformal contact of rail and wheel, the contact area is approximated by a plane, making it appropriate to use Boussinesq's influence function for all surfaces. However, in conformal contact (where the contact surface is not approximately plane), it is generally necessary to find more individualized influence functions for each of the two surfaces in contact. For many realistic surfaces, the exact influence functions cannot be found analytically; therefore, they must be generated numerically [Woodward and Paul, 1976], or else be approximated by some convenient mathematical expresssions.

A study of various exact and approximate influence functions has been made by Hashemi and Paul[1979]. Although, in principle, one may generate accurate influence functions for arbitrary surface geometries with the aid of three-dimensional finite element programs, their studies indicate that the costs of such an approach for rail and wheel geometries are prohibitive at this time. However, they have found that it is feasible to use various types of semi-empirical influence functions and have made error analyses which indicate that the Boussinesq influence function [Lur'e, 1964] is a reasonable first approximation for the range of wheel and rail geometries encompassed in the examples of this paper. That is, the normal displacement w_n at a point (x,y,z) of the wheel or rail surface, due to a unit normal force at another point (x',y',z') of the surface may be approximated by:

$$w_n = \frac{(1-\nu)/\pi E)}{[(x-x')^2+(y-y')^2+(z-z')^2]^{1/2}}$$

where E and ν are Young's modulus and Poisson's ratio, for the body in question. This was the influence function used by CONFORM in the examples of this report.

LIST OF RELATED REPORTS AND PUBLICATIONS

A. FRA Technical Reports (Available from National Technical Information Service)

A1. Paul, B., "A Review of Rail-Wheel Contact Stress Problems," Technical Report No. 1, April 1975, FRA/ORD-76 141, PB 251238/AS, Contract DOT-OS-40093.

A2. Woodward, W., and Paul, B., "Contact Stresses for Closely Conforming Bodies - Application to Cylinders and Spheres," Technical Report No. 2, December 1976, DOT/TST/77-48, PB 271033/AS, Contract DOT-OS-40093.

A3. Paul, B., and Hashemi, J., "An Improved Numerical Method for Counterformal Contact Stress Problems," Technical Report No. 3, July 1977, FRA/ORD-78/26, Contract DOT-OS-60144, PB 286228/AS.

A4. Paul, B., and Hashemi, J., "User's Manual for Program COUNTACT COUNTerformal contACT stress problems ", Technical Report No. 4, September 1977, FRA/ORD-78/27, Contract DOT-OS-60144, PB 286097/AS.

A5. Paul, B., and Hashemi, J., "User's Manual for Program CONFORM (CONFORMal contact stresses between wheels and rails ", Technical Report No. 5, June 1978 FRA/ORD-78/40, Contract DOT-OS-60144, PB 288927/AS.

A6. Paul, B., and Hashemi, J., "Rail-Wheel Geometry Associated with Contact Stress Analysis," Technical Report No. 6, 1978, FRA/ORD-78/41, Contract DOT-OS-60144, (to be issued).

A7. Paul, B., and Hashemi, J., "Contact Stresses in Bodies with Arbitrary Geometry, Applications to Wheels and Rails," Technical Report No. 7, April 1979, FRA/ORD/79-23, Contract DOT-OS-60144.

A8. Paul, B., and Hashemi, J., "Numerical Determination of Contact Pressures Between Closely Conforming Wheels and Rails", Technical Report No. 8. July, 1979, FRA/ORD-79/41, Contract DOT-OS-60144.

B. Related Papers Published in Various Journals and Proceedings

B1. Singh, K. P., and Paul, B., "A Method for Solving Ill-Posed Integral Equation of the First Kind," Computer Methods in Applied Mechanics and Engineering, Vol. 2, 1973, 339-348.

B2. Singh, K. P., and Paul, B.,"Numerical Solution of Non-Hertzian Elastic Contact Problems," Journal of Applied Mechanics, Vol. 41, Trans. of ASME, Series E, Vol. 96, June 1974, pp. 484-490.

B3. Singh, K. P., and Paul, B., "Stress Concentration in Crowned Rollers," Journal of Engineering for Industry, Trans. ASME, Series B, Vol. 97, No. 3, 1975, pp. 990-994.

B4. Paul, B., K. P. Singh., and Woodward, W., "Contact Stresses for Multiply-Connected Regions--The Case of Pitted Spheres," Proceedings of the Symposium on the Mechanics of Deformable Bodies, Delft University Press, 1975, pp. 264-281.

B5. Paul, B., "A Review of Rail-Wheel Contact Stress Problems," in Proceedings of Symposium on Railroad Track Mechanics, Pergamon Press, 1978, Ed. by A. Kerr, pp. 323-351.(Based on Ref. A1).

B6. Paul, B., and Hashemi, J., "An Improved Numerical Method for Counterformal Contact Stress Problems," in Computational Techniques for Interface Problems, AMD-Vol, 30, Ed. by K. C. Park and D. K. Gartlung, American Society of Mechanical Engineers, N.Y., 1978, pp. 165-180. (Same as Ref. A3).